*The Journal of* **Immunology**

# Cutting Edge: Regulation of Exosome Secretion by the Integral MAL Protein in T Cells

This information is current as of September 18, 2015.

Leandro N. Ventimiglia, Laura Fernández-Martín, Emma Martínez-Alonso, Olga M. Antón, Milagros Guerra, José Angel Martínez-Menárguez, Germán Andrés and Miguel A. Alonso

|  |  |
|---|---|
| **Supplementary Material** | http://www.jimmunol.org/content/suppl/2015/06/23/jimmunol.1500891.DCSupplemental.html |
| **References** | This article **cites 16 articles**, 5 of which you can access for free at: http://www.jimmunol.org/content/195/3/810.full#ref-list-1 |
| **Subscriptions** | Information about subscribing to *The Journal of Immunology* is online at: http://jimmunol.org/subscriptions |
| **Permissions** | Submit copyright permission requests at: http://www.aai.org/ji/copyright.html |
| **Email Alerts** | Receive free email-alerts when new articles cite this article. Sign up at: http://jimmunol.org/cgi/alerts/etoc |

# Cutting Edge: Regulation of Exosome Secretion by the Integral MAL Protein in T Cells

Leandro N. Ventimiglia,* Laura Fernández-Martín,* Emma Martínez-Alonso,[†]
Olga M. Antón,* Milagros Guerra,[‡] José Angel Martínez-Menárguez,[†]
Germán Andrés,[‡] and Miguel A. Alonso*

Exosomes secreted by T cells play an important role in coordinating the immune response. HIV-1 Nef hijacks the route of exosome secretion of T cells to modulate the functioning of uninfected cells. Despite the importance of the process, the protein machinery involved in exosome biogenesis is yet to be identified. In this study, we show that MAL, a tetraspanning membrane protein expressed in human T cells, is present in endosomes that travel toward the plasma membrane for exosome secretion. In the absence of MAL, the release of exosome particles and markers was greatly impaired. This effect was accompanied by protein sorting defects at multivesicular endosomes that divert the exosomal marker CD63 to autophagic vacuoles. Exosome release induced by HIV-1 Nef was also dependent on MAL expression. Therefore, MAL is a critical element of the machinery for exosome secretion and may constitute a target for modulating exosome secretion by human T cells. *The Journal of Immunology*, 2015, 195: 810–814.

The term exosome applies to membranous vesicles of endosomal origin with a diameter of 40–100 nm that are released into the extracellular space. Exosomes are currently considered to be vehicles that transfer biomolecules to recipient cells to modulate their activity (1). HIV-1 usurps the exosome-based intercellular communication network of T cells to render quiescent T cells permissive to HIV-1 replication (2, 3). Exosomes from regulatory T cells can suppress effector T cells by delivering microRNAs via exosomes (4). These findings suggest that modulation of the exosome route in T cells may be of therapeutic value for preventing T cell–mediated diseases such as inflammation or for interfering with the progression of HIV-1 infection (5, 6).

Exosomes are generated as intraluminal vesicles (ILV) in multivesicular endosomes (MVE). Additionally, MVE contain ILV that are to be delivered to lysosomes (7). The endosomal sorting complex responsible for transport (ESCRT) is responsible for ILV formation and cargo sorting in the endo-lysosome route (8) and for exosome secretion in some (9), but not in all (10), cell types. Release of the exosomal marker CD63 in Jurkat T cells is dependent on ceramide but independent of Hrs (11), which is a component of the ESCRT machinery. Despite the interest from a fundamental point of view and in the applications that might stem from it, the identity of the components of the protein machinery underlying the process of exosome secretion in T cells remains a mystery.

MAL is a 17-kDa tetraspanning membrane protein known to be essential for specialized routes of protein transport to the plasma membrane and the organization of the immunological synapse in human T cells (12, 13). The work reported in the present study addresses the role of MAL in exosome secretion in Jurkat T cells.

## Materials and Methods

### Reagents

The mAb 6D9 to human MAL has been described elsewhere (14). The sources of the Abs to the indicated proteins used were as follows: CD59 from Abcam, CD63 from the Developmental Studies Hybridoma Bank (DSHB), tsg101 from Santa Cruz Biotechnology, calnexin from Stressgen. Fluorescent Alexa–conjugated secondary Abs were obtained from Invitrogen. HRP-conjugated secondary Abs were from Jackson ImmunoResearch Laboratories.

### DNA constructs and transfection conditions

The DNA constructs expressing MAL-cherry and short hairpin (sh)RNA to MAL have been described elsewhere (12, 13). The DNA construct expressing MAL mRNA lacking 5′ and 3′ untranslated regions designed to be insensitive to shMALa expression was made in the pCDNA3.1 Zeo vector (Invitrogen). The DNA constructs expressing Nef-GFP and Rab5-Q79L-GFP (Addgene plasmid 35140) were gifts from A. Alcover (Institut Pasteur, Paris, France) and S. Grinstein (Hospital for Sick Children, Toronto, ON, Canada). For stable transfection, Jurkat cells were selected with the 1 mg/ml G418 or 1 μg/ml Zeocin, cloned by limiting dilution. The resulting clones were screened by immunoblotting with anti-MAL mAb 6D9.

*Departamento de Biología Celular e Inmunología, Centro de Biología Molecular Severo Ochoa, Consejo Superior de Investigaciones Científicas, Universidad Autónoma de Madrid, Cantoblanco, 28049 Madrid, Spain; [†]Departamento de Biología Celular e Histología, Facultad de Medicina, Instituto Murciano de Investigación Biosanitaria, Universidad de Murcia, 30100 Murcia, Spain; and [‡]Unidad de Microscopía Electrónica, Centro de Biología Molecular Severo Ochoa, Consejo Superior de Investigaciones Científicas, Universidad Autónoma de Madrid, Cantoblanco, 28049 Madrid, Spain

Address correspondence and reprint requests to Prof. Miguel A. Alonso, Centro de Biología Molecular Severo Ochoa, Nicolas Cabrera 1, 28049 Madrid, Spain. E-mail address: maalonso@cbm.csic.es

The online version of this article contains supplemental material.

Abbreviations used in this article: ESCRT, endosomal sorting complex responsible for transport; ILV, intraluminal vesicle; KD, knockdown; MVE, multivesicular endosome; sh, short hairpin.

## Isolation and analysis of exosomal fractions

To isolate the 100,000 × g exosomal fraction of Jurkat cells by differential centrifugation or by centrifugation to equilibrium we followed standard protocols (15). Samples were subjected to SDS-PAGE and processed for immunoblotting. Band intensities were quantified using ImageJ software, and results were expressed relative to the control condition.

## Quantification of the number of exosome particles

Aliquots of the resuspended 100,000 × g exosomal pellet of control and MAL knockdown (KD) cells were deposited on EM grids and processed for whole-mounted analysis under an electron microscope following an established protocol (15). Images taken from different fields were then systematically analyzed for the presence of 40- to 100-nm vesicles.

## Immunofluorescence analysis

Cells were fixed in formalin for 30 min, rinsed, and treated with 10 mM glycine in PBS for 5 min. Immunofluorescence analysis was carried out as described elsewhere (12). For time-lapse fluorescence microscopy, cells were plated onto fibronectin-coated chambers and imaged using an AF6000 LX microscope (Leica). Brightness and contrast were optimized with Adobe Photoshop CS6 software. Quantifications were performed using ImageJ software.

## Correlative light-electron microscopy

Jurkat cells expressing CD63-GFP attached to gridded glass-bottom dishes were fixed with 4% paraformaldehyde. Selected cells expressing CD63-GFP were visualized by z-stack imaging (optical section, 300 nm) using a Zeiss L510 laser confocal microscope. Phase contrast light microscopy was used to map the position of the selected cells on the gridded coverslip. Cells were further fixed with 2% glutaraldehyde followed by 2% osmium tetroxide. After Epon embedding, cells were ultrasectioned entirely along their z-axis into serial 80-nm-thick sections, which were poststained with uranyl acetate and lead citrate. Samples were then examined at 80 kV in a Jeol JEM-1010 electron microscope. Selected fluorescent images exhibiting multiple CD63⁺ spots were mapped onto the corresponding electron microscopy sections by overlapping them manually with the help of Adobe Photoshop CS6.
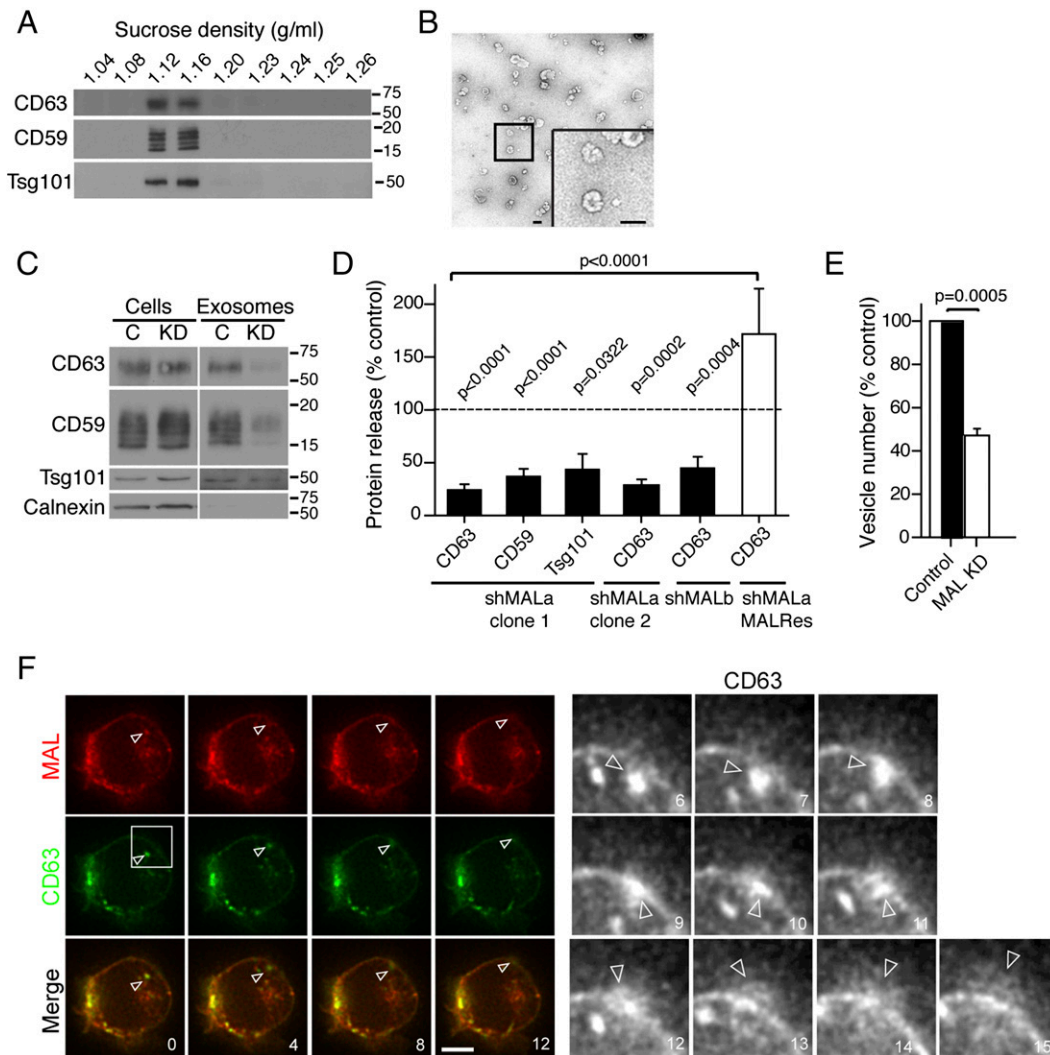


**FIGURE 1.** MAL is required for constitutive exosome secretion. (**A**) The exosomal 100,000 × g pellet fraction was centrifuged to equilibrium in a 2.0–0.25 M sucrose density gradient. Aliquots from the different fractions were analyzed by immunoblotting with the indicated Abs. (**B**) Electron microscopy image of a whole-mount exosomal sample from control cells stained with uranyl acetate. The inset shows the boxed region at higher magnification. Scale bars, 100 nm. (**C**) Total cell extracts (*left*) and exosome fractions (*right*) from equal numbers of cells from control cells or cells stably silenced for MAL with shMALa were immunoblotted for the indicated proteins. (**D**) Levels of CD63, CD59, and tsg101 represented as the percentage relative to control cells in the exosome fraction of wild-type cells silenced for MAL with shMALa cell clones 1 and 2 or shMALb and in cells stably expressing exogenous MAL resistant to shMALa expression (shMALa MALRes). The broken line indicates 100% secretion of each of the proteins analyzed in the control cells. (**E**) The numbers of 40- to 100-nm vesicles in electron microscopy images of whole-mount exosome samples from control and MAL KD cells were quantified. Approximately 900 and 450 vesicles with these characteristics were identified in the samples from control cells and MAL KD cells, respectively, upon analysis of the same number of images. (**F**) Cells coexpressing MAL-cherry and CD63-GFP were examined by time-lapse videomicroscopy. The arrowhead indicates a vesicle positive for both MAL and CD63 that fuses with the plasma membrane and discharges its contents. Scale bar, 5 μm. An enlargement of the boxed region is shown on the right for CD63-GFP. The contrast of the enlarged images was adjusted to show the fusion event and the material released into the extracellular space more clearly. Scale bar, 1 μm. Numbers indicate time in seconds. Means ± SEM of three independent experiments are shown in (D) and (E).

*Statistical analysis*

Data are expressed as the means ± SEM. A Student *t* test was used to calculate the statistical significance of differences between group means.

## Results and Discussion

To analyze exosome secretion by Jurkat cells, we chose CD63, CD59, and tsg101 as being representative of tetraspanins, GPI-anchored proteins, and the ESCRT machinery, respectively. To characterize the exosomes, the fraction obtained by differential centrifugation of the culture medium was centrifuged in a sucrose density gradient. The three exosomal markers showed clear enrichment in the 1.12 and 1.16 g/ml fractions (Fig. 1A). The exosomes had the size and typical collapsed morphology (Fig. 1B) reported for exosomes analyzed as whole-mount samples (1). Therefore, according to their density, morphology, and size, the vesicles isolated by differential centrifugation are enriched in bona fide exosomes.

We generated cell clones stably silenced for MAL expression using two shRNAs (shMALa and shMALb). These cell clones, which immunoblotting assays revealed their endogenous MAL levels to be reduced reduced by >98% (Supplemental Fig. 1A), were then used to compare the release of the exosome markers. A drop in exosome marker secretion was observed in cells knocked down for MAL expression with shMALa, clones 1 and 2, and small interfering MALb. However, this was not apparent in shMALa KD cells expressing exogenous MAL that was resistant to small interfering MALa (MALRes) (Fig. 1C, 1D). As a control we observed that the total cellular content of the markers was not altered by the absence of MAL expression in shMALa clone 1 cells, which we subsequently refer to as MAL KD cells (Supplemental Fig. 1B). Consistent with the reduced secretion of the markers, it is of note that exosomes were secreted in small amounts by MAL KD cells, taken as the number of 40- to 100-nm vesicles secreted by equal numbers of cells, measured under an electron microscope (Fig. 1E). The total protein content in the exosome pellet of MAL KD cells, determined by the Bradford assay, was ~50% of that in control cells. Because the $100,000 \times g$ pellet almost certainly contains other types of material (e.g., apoptotic bodies, shedding vesicles), this decrease may well account for the block observed in the number of exosomes in MAL KD cells (Fig. 1E).

We took CD63 to be representative of exosome cargo and coexpressed CD63-GFP and MAL-cherry to analyze the dynamics of MAL and CD63 simultaneously by time-lapse
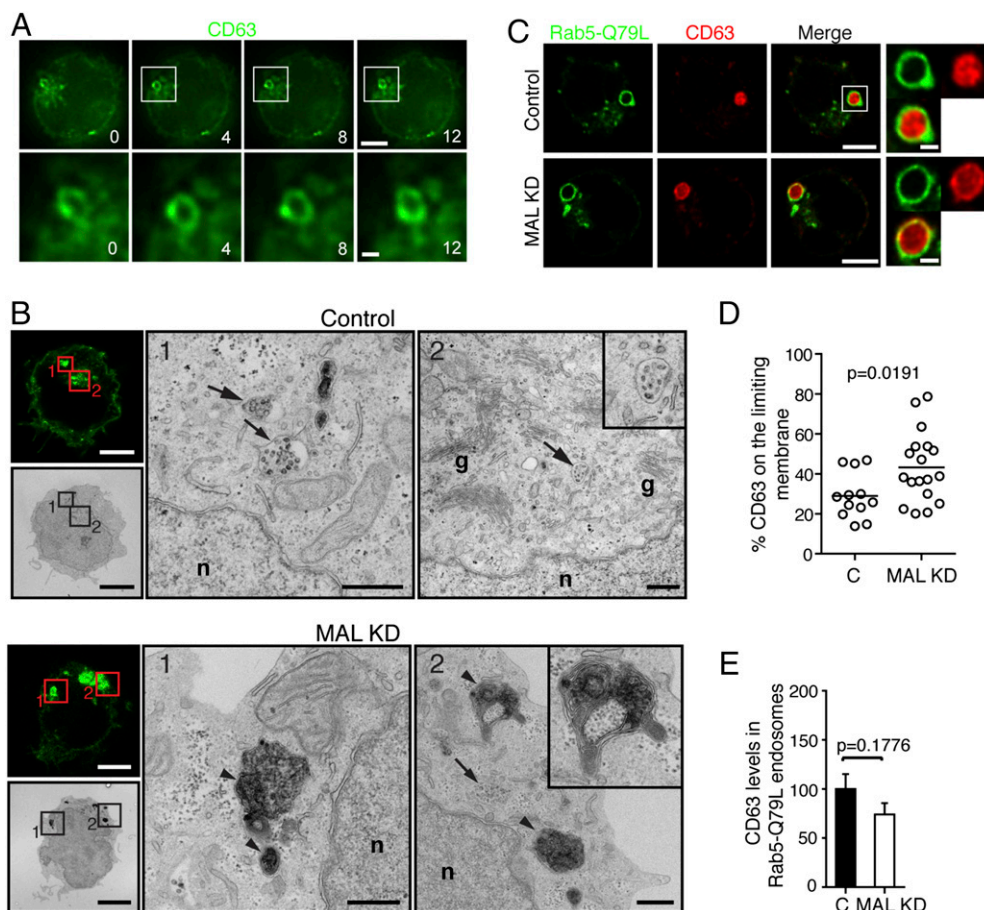
**FIGURE 2.** MAL silencing diverts CD63 to autophagic vacuoles and lysosomes. (**A**) MAL KD cells expressing CD63-GFP cells were examined by time-lapse video-microscopy. Scale bars, 5 μm. An enlargement of the boxed region is shown. Scale bar, 1 μm. Numbers indicate time in seconds. (**B**) Control (*top panels*) and MAL KD (*bottom panels*) cells transiently expressing CD63-GFP were fixed and processed for correlative light-electron microscopy analysis. The *left panels* show the confocal section and the equivalent physical section. Scale bars, 5 μm. The boxed regions are shown at higher magnification. Scale bars, 500 nm. The arrows point to MVE and the arrowheads to lysosomes and autophagic vacuoles. g, Golgi; n, nucleus. (**C–E**) Control or MAL KD cells transiently expressing Rab5-Q79L-GFP were stained for CD63. A confocal plane is shown. Scale bars, 5 μm. An enlargement of the boxed areas is shown. Scale bars, 1 μm (C). The histograms represent the percentage of CD63 in the limiting membrane relative to the total content in each individual Rab5-Q79L+ endosome analyzed (D), and the total content of CD63 in individual Rab5-Q79L endosomes in MAL KD cells is expressed as the percentage relative to that in control cells (E). Three independent experiments were performed. Means ± SEM are shown in (E).
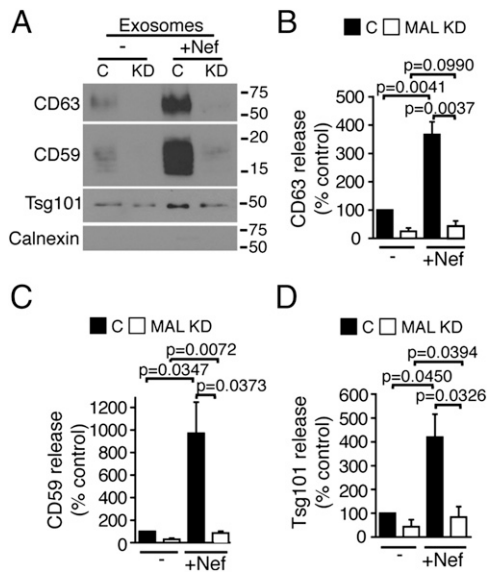
**FIGURE 3.** HIV-1 Nef exploits the MAL-dependent pathway for stimulation of exosome release. (**A–D**). The exosome fraction of cells transfected with Nef-GFP was immunoblotted for the indicated proteins (A). Given the strong signal intensity of the CD63 and CD59 bands in the lanes corresponding to control cells overexpressing Nef-GFP, the immunoblots of these two proteins were underexposed relative to those shown in Fig. 1C. The histograms represent the levels of CD63 (B), CD59 (C), and tsg101 (D) in the exosome fraction of MAL KD cells represented as the percentage relative to untransfected control cells. Three independent experiments were performed. Means ± SEM are shown in (B)–(D).

videomicroscopy. We detected endosome structures that were positive for both proteins. Occasionally, we observed that these endosomes moved toward the plasma membrane and discharged their content into the extracellular space, leaving a halo of secreted CD63+ exosomes (Fig. 1F, Supplemental Video 1). In summary, MAL, which is present with exosomal cargo in the same endosomes that travel to the plasma membrane for exosome secretion, is required for the release of exosomes.

When we compared the dynamics of CD63 in MAL KD cells (Fig. 2A, Supplemental Video 2) with that of control cells (Fig. 1F, Supplemental Video 1), the most obvious effect of MAL KD was the accumulation of CD63 in apparently large intracellular structures that moved erratically and were unable to fuse with the plasma membrane. These structures were characterized by correlative light-electron microscopy as being lysosomes and autophagic vacuoles (Fig. 2B). We used Rab5-Q79L expression as a tool to generate large MVE, which facilitate the analysis of the role of MAL in sorting CD63 to ILV. It is of particular note that, consistent with the impairment of the secretion of CD63 and with its presence in autophagic vacuoles, CD63 showed ∼14% missorting to the limiting membrane in MAL KD cells (Fig. 2C, 2D). Because exosome secretion was inhibited in MAL KD cells, the missorted pool of CD63 might reflect the population of CD63+ ILV normally destined for secretion in exosomes, whereas the luminal CD63 would correspond to the pool of ILV normally destined for fusion with lysosomes. As a control, we observed that the levels of CD63 in enlarged Rab5-Q79L+ MVE were similar in control and MAL KD cells (Fig. 2E). We conclude that MAL is necessary for the efficient fusion of endosomes with the plasma membrane so that they can discharge their ILV content into the extracellular space in

the form of exosomes, and for correctly sorting the exosomal cargo in MVE.

Expression of the HIV-1 accessory protein Nef in T cells induces massive secretion of exosome markers (16, 17). We examined whether Nef targets the MAL-dependent route. The percentage of Nef-transfected cells and the levels of Nef expression were similar in control and MAL KD cells (Supplemental Fig. 2). Consistent with a previous report (17), Nef induced secretion of all the exosome markers analyzed. It is of note that Nef could not overcome the block on exosome marker secretion imposed by MAL KD (Fig. 3). These findings indicate that HIV-1 Nef induces exosome marker secretion by exploiting the MAL-mediated constitutive route of exosome biogenesis. Bearing in mind that exosome particle secretion is inhibited in MAL KD cells (Fig. 1E), it is reasonable to suppose that the drastic reduction of exosome marker release observed in Nef-transfected MAL KD cells is due to deficient exosome biogenesis.

Exosome modulation has the therapeutic potential to fight T cell–mediated diseases and HIV-1 infection (2–6). Our results point to the integral MAL protein being a key element of the protein machinery for exosome secretion and a candidate protein target for modulating exosome release in human T cells.

## Acknowledgments

## Disclosures

The authors have no financial conflicts of interest.

## References

1. Raposo, G., and W. Stoorvogel. 2013. Extracellular vesicles: exosomes, microvesicles, and friends. *J. Cell Biol.* 200: 373–383.
2. Arenaccio, C., C. Chiozzini, S. Columba-Cabezas, F. Manfredi, E. Affabris, A. Baur, and M. Federico. 2014. Exosomes from human immunodeficiency virus type 1 (HIV-1)-infected cells license quiescent CD4+ T lymphocytes to replicate HIV-1 through a Nef- and ADAM17-dependent mechanism. *J. Virol.* 88: 11529–11539.
3. Arenaccio, C., C. Chiozzini, S. Columba-Cabezas, F. Manfredi, and M. Federico. 2014. Cell activation and HIV-1 replication in unstimulated CD4+ T lymphocytes ingesting exosomes from cells expressing defective HIV-1. *Retrovirology* 11: 46.
4. Okoye, I. S., S. M. Coomes, V. S. Pelly, S. Czieso, V. Papayannopoulos, T. Tolmachova, M. C. Seabra, and M. S. Wilson. 2014. MicroRNA-containing T-regulatory-cell-derived exosomes suppress pathogenic T helper 1 cells. *Immunity* 41: 89–103.
5. Agarwal, A., G. Fanelli, M. Letizia, S. L. Tung, D. Boardman, R. Lechler, G. Lombardi, and L. A. Smyth. 2014. Regulatory T cell-derived exosomes: possible therapeutic and diagnostic tools in transplantation. *Front. Immunol.* 5: 555.
6. Zhang, B., Y. Yin, R. C. Lai, and S. K. Lim. 2014. Immunotherapeutic potential of extracellular vesicles. *Front. Immunol.* 5: 518.
7. Hanson, P. I., and A. Cashikar. 2012. Multivesicular body morphogenesis. *Annu. Rev. Cell Dev. Biol.* 28: 337–362.
8. Wollert, T., and J. H. Hurley. 2010. Molecular mechanism of multivesicular body biogenesis by ESCRT complexes. *Nature* 464: 864–869.
9. Baietti, M. F., Z. Zhang, E. Mortier, A. Melchior, G. Degeest, A. Geeraerts, Y. Ivarsson, F. Depoortere, C. Coomans, E. Vermeiren, et al. 2012. Syndecan-syntenin-ALIX regulates the biogenesis of exosomes. *Nat. Cell Biol.* 14: 677–685.
10. Trajkovic, K., C. Hsu, S. Chiantia, L. Rajendran, D. Wenzel, F. Wieland, P. Schwille, B. Brügger, and M. Simons. 2008. Ceramide triggers budding of exosome vesicles into multivesicular endosomes. *Science* 319: 1244–1247.
11. Mittelbrunn, M., C. Gutiérrez-Vázquez, C. Villarroya-Beltri, S. González, F. Sánchez-Cabo, M. A. González, A. Bernad, and F. Sánchez-Madrid. 2011. Unidirectional transfer of microRNA-loaded exosomes from T cells to antigen-presenting cells. *Nat. Commun.* 2: 282.
12. Antón, O., A. Batista, J. Millán, L. Andrés-Delgado, R. Puertollano, I. Correas, and M. A. Alonso. 2008. An essential role for the MAL protein in targeting Lck to the plasma membrane of human T lymphocytes. *J. Exp. Med.* 205: 3201–3213.

13. Antón, O. M., L. Andrés-Delgado, N. Reglero-Real, A. Batista, and M. A. Alonso. 2011. MAL protein controls protein sorting at the supramolecular activation cluster of human T lymphocytes. *J. Immunol.* 186: 6345–6356.

14. Millán, J., and M. A. Alonso. 1998. MAL, a novel integral membrane protein of human T lymphocytes, associates with glycosylphosphatidylinositol-anchored proteins and Src-like tyrosine kinases. *Eur. J. Immunol.* 28: 3675–3684.

15. Théry, C., S. Amigorena, G. Raposo, and A. Clayton. 2006. *Isolation and Characterization of Exosomes from Cell Culture Supernatants and Biological Fluids.* Wiley, New York.

16. Muratori, C., L. E. Cavallin, K. Krätzel, A. Tinari, A. De Milito, S. Fais, P. D'Aloja, M. Federico, V. Vullo, A. Fomina, et al. 2009. Massive secretion by T cells is caused by HIV Nef in infected cells and by Nef transfer to bystander cells. *Cell Host Microbe* 6: 218–230.

17. Lenassi, M., G. Cagney, M. Liao, T. Vaupotič, K. Bartholomeeusen, Y. Cheng, N. J. Krogan, A. Plemenitaš, and B. M. Peterlin. 2010. HIV Nef is secreted in exosomes and triggers apoptosis in bystander CD4+ T cells. *Traffic* 11: 110–122.